Journal of Archaeological Science: Reports 69 (2026) 105540

Contents lists available at ScienceDirect

Journal of Archaeological Science: Reports

journal homepage: www.elsevier.com/locate/jasrep

Using high energy X-ray imaging to reveal the internal structure of bronze-hilted Iron swords

Yui Arimatsu

Hiroshima University, 1-2-3 Kagamiyama, Higashi-Hiroshima, Hiroshima 739-0046, Japan

ARTICLE INFO

Keywords:
High energy X-ray imaging
Iran
Caucasus
Bimetal
Iron adoption

ABSTRACT

Bronze-hilted iron swords excavated from northern Iran to the South Caucasus are considered the earliest iron tools discovered in these regions. These swords are important for understanding the adoption of iron in these regions, partly because of the possibility that the iron tangs remain inside the hilts without rusting. However, the details of the iron tangs and production techniques, including the method for combining iron and bronze, remain unclear. It is necessary to examine the internal structure of the bronze hilts. Tomography imaging has been attempted, but no concrete findings were achieved. This study utilized high-resolution X-ray imaging techniques, including three-dimensional Computed Tomography, to analyze the internal structure of bronze-hilted iron swords. This enabled the identification of the unique features of their internal structures, which appeared to differ according to pommel type. These techniques illuminated the limitations of early iron metalworking, the techniques used for bronze casting, and the trial-and-error process involved in these developments. These results indicate the efficacy of these imaging methods and suggest fruitful directions for further research on similar archaeological materials.

1. Introduction

Multiple bronze-hilted iron swords combining an iron blade with a bronze hilt have been excavated in northwestern Iran and the South Caucasus (de Morgan, 1927; Gambaschidze et al., 2001; Kuftin, 1941; Medvedskaya, 1982; Nieling, 2009; Wever, 1969) (Fig. 1). These swords have been categorized into several types based on the design of the pommels. The most well-known is referred to as an "ear pommel" (split-ear pommel or saddle-shaped pommel; Figs. 2-1, 2-2). Bronze-hilted iron swords with ear pommels have been found in the mountainous areas of northwestern Iran (Thornton and Pigott, 2011, Fig. 6.24) and the inland area of the South Caucasus (Gambaschidze et al., 2001, 406; Kuftin, 1941, Figs. 59, 60). Swords with a "cotton-reel pommel" (Figs. 2-3, 2-4) have been excavated on the coasts of the Caspian Sea, primarily along the western (Khalatbari, 2004, Figs. 50–52; Medvedskaya, 1982, Figs. 9–28, 9–29) and southern coasts (Fukai and Ikeda, 1971, 26, Pl. XLIV-1). Ear pommel-type swords have also been excavated on the Sea's western coast (Khalatbari, 2004, Fig. 53; Medvedskaya, 1982, Fig. 9–30). Several other types of bronze-hilted iron swords have also been excavated in this region (Khalatbari, 2004, Figs. 50, 51), suggesting that this region was a hub for the distribution and exchange of a variety of swords during the period.

Bronze-hilted iron swords are regarded as important archaeological evidence from the early Iron Age in Iran (Pigott, 1981, 2004). They are among the earliest iron artifacts discovered in the region. In northern Iran, iron tools are considered to have been adopted from the ninth century BC onwards (Danti, 2013). In this context, bronze-hilted iron swords have been given a relative date of around the thirteenth to mid-eighth century BC (Hajitabar and Haji, 2022; Khalatbari, 2004, 84; Maxwell-Hyslop and Hodges, 1962; Medvedskaya, 1982, 76; Moorey, 1974; Nojima et al., 2016; Pigott, 1999). In addition to their chronological context, their incorporation of both metals makes them an effective source for clarifying the relationship between bronze and iron production during the transitional phase.

Early ironwork was carried out in the same workplaces as bronze production (Eliyahu-Behar et al., 2012; Erb-Satullo et al., 2020; Pigott, 1989; Yahalom-Mack and Eliyahu-Behar, 2015, 299). Investigating the metallurgical techniques used in the swords will therefore contribute to understanding this relationship (Pigott, 1989, 73–74). Furthermore, the swords likely have iron tangs remaining inside the bronze hilt that have been protected from rusting, as many have been proved to be magnetized from the grips to the pommels (Nojima et al., 2016; Rodzinka et al., 2024). The future analysis of iron tangs from materials with clear provenience would allow a closer understanding of early ironwork (Nojima

E-mail address: yarima@hiroshima-u.ac.jp.

https://doi.org/10.1016/j.jasrep.2025.105540
Received 24 July 2025; Received in revised form 3 November 2025; Accepted 4 December 2025
Available online 9 December 2025

et al., 2016, 21–22; Rodzinka et al., 2024, 13).

Other bimetal tools from the earliest phase of iron adoption have been excavated in Cyprus and the Levant (Erb-Satullo, 2019, 566; Waldbaum, 1982; Yahalom-Mack and Eliyahu-Behar, 2015, 288–289). However, these were iron knives with bronze rivets. Meanwhile, the bronze-hilted iron swords from northern Iran and the South Caucasus feature iron parts within a bronze casting. These two types of bimetal objects may represent fundamentally different technological traditions. In the area of bronze-hilted iron swords, a different process of adoption of iron may have undergone, compared to the Mediterranean coastal region. These swords may provide a new perspective on the adoption process of iron artifacts and serve as clues to clarifying this process.

The bronze-hilted iron swords of northern Iran and the South Caucasus are therefore important artifacts that could shed light on the process of the adoption of iron in West Asia. A more in-depth analysis of the materials and the metalworking techniques will contribute to a detailed understanding of the adoption of iron and its incorporation into metallurgy in northern Iran and the South Caucasus. However, few findings have managed to illuminate these production techniques. A comprehensive study examined metal artifacts produced by overlaying and bonding additional metal onto mental components, inferring their manufacturing processes (Drescher, 1958). The study described daggers and knives combining iron blades with bronze hilts (ibid., 75, 81–84, Taf. 15, Taf. 18), noting several examples where blades were cast into hilts rather than inserted (ibid., 82). Based on these findings, bronze-hilted iron swords excavated from Hasanlu in northwestern Iran are presumed to have been produced through lost-wax casting (Pigott, 1989, 72–73).

This study provides a valuable reference for understanding manufacturing techniques of bimetallic artifacts. However, it primarily focuses on artifacts from Western and Northern Europe, which differ morphologically from bronze-hilted iron swords of Western Asia and the South Caucasus. Moreover, some artifacts' production were deemed too complex to reconstruct, with Drescher (1958, 4–5, 76, 81) acknowledging the necessity of further data, including X-ray imaging, to clarify these methods. Consequently, direct evidence substantiating the production processes of bimetallic swords from Western Asia remains limited, with detailed examinations and data on their manufacturing techniques rarely presented. Consequently, regional variations in techniques, differences among pommel types, and their chronological changes also remain unclear.

One reason for this limitation, as discussed below, is the absence of an established methodology for non-destructive analysis. This study therefore used contemporary high-energy X-ray imaging methods, including three-dimensional Computed Tomography (3DCT), to present an effective non-destructive approach for analyzing the internal structure of the hilts. The results further demonstrated the wide applicability of X-ray technologies in the archaeological field and allowed the construction of hypotheses on the production techniques and their variations.

2. Background

Nondestructive imaging has previously been conducted of the inside of the hilts of bronze-hilted iron swords. In most cases, little or nothing of the iron blades survive, much like other ancient iron artifacts. To gain

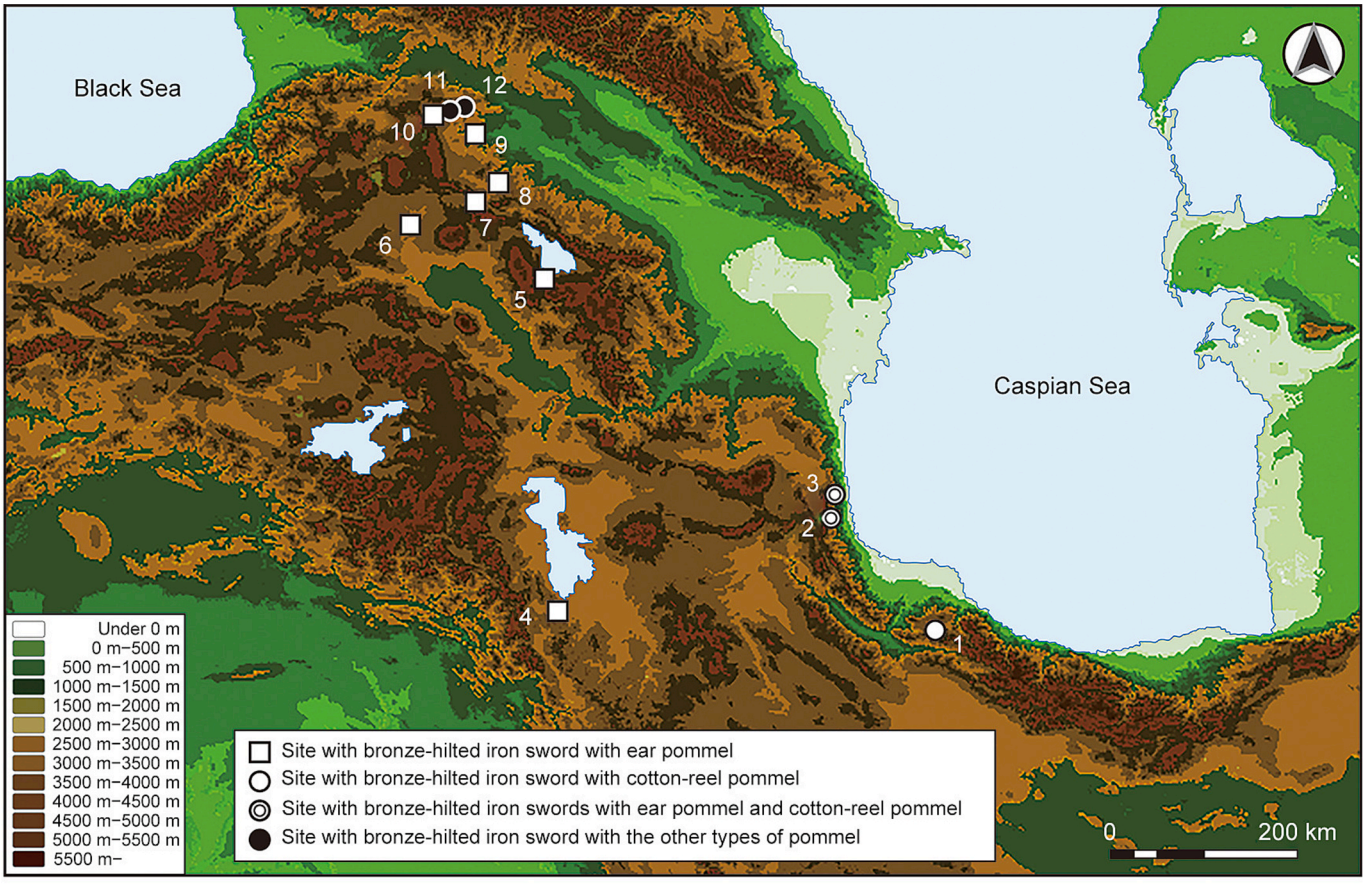

Fig. 1. Major sites for bronze-hilted iron swords with ear and cotton-reel pommels in Iran and Transaucasia (created by the author based on de Morgan 1927; Fukai and Ikeda, 1971; Gambaschidze et al., 2001; Khalatbari, 2004; Kuftin, 1941; Medvedskaya, 1982; Nieling, 2009).

further insight into ancient iron and its production technics, the internal structure of the hilt—housing the only possible remaining iron—therefore must be understood. Since the 2010s, tomographic imaging of the hilts has been possible, including X-ray (Simpson and La Niece, 2010) and gamma ray imaging (Shizuma et al., 2017). However, the resolution of the images was still insufficient for comprehending the internal structure and reconstructing the production techniques. Bronze-hilted iron swords are large, thick objects made of multiple heavy metals. Due to their low transparency and appearance of artifacts on images, it is difficult to obtain adequate image data for analysis. In recent years, neutron tomography has been applied in this capacity. For example, Rodzinka et al. (2024) focused on ear pommel-type swords that appeared to be completely bronze. The imaging results clearly revealed that areas around the guards and inside grips had been tampered with in modern times. However, they also indicated possible iron tangs remaining within the bronze hilts. Similar results have been found by other studies (e.g., Kontani, 2001, 2005; Kontani and Tanaka, 2002; Nojima et al., 2016). The results of neutron imaging have confirmed these findings by providing details of later modifications. However, the details from the unmodified areas were still not clear (Rodzinka et al., 2024). Neutron imaging is therefore not enough to observe the morphology of the iron tang, its potential rusting, or metal remains. The conditions of the hilts inside the casting that would permit the reconstruction of casting techniques thus remained unknown.

In this context, high-energy X-ray imaging has demonstrated its effectiveness. Bronze-hilted iron swords have been imaged using 200 keV (keV) X-rays at the Super Photon Ring – 8 GeV (SPring-8) large synchrotron radiation facility (Hoshino et al., 2017; Okayama Orient Museum et al., 2021). The results clearly showed the shape of the iron tang inside the hilt and the metals (Hoshino et al., 2017, Fig. 7; Okayama Orient Museum et al., 2017, Figs. 2, 3). Interestingly, these images have indicated variations in the internal structure (cf. Okayama Orient Museum et al., 2017, Figs. 2, 3). However, the details, including the materials for imaging and the image data, have not been published and there has been little explanation of the individual images. Therefore, the relationship between variations in internal structure and pommel type is still unavailable, and comprehensive insights into the swords using these findings are impossible. This study addressed this gap by conducting high-energy X-ray imaging on bronze-hilted iron swords with the express purpose of creating a detailed analysis of the internal structure of the swords and their variations.

3. Materials and methods

3.1. Materials

The artifacts analyzed in this study were four bronze-hilted iron swords (Nos. 509, 510, 512, 513) kept at the Institute for Research in Humanities (*Jinbunken*) at Kyoto University. These were acquired in Iran in 1959 by the Kyoto University scientific mission to the Iranian Plateau and Hindukush under Mizuno Seiichi. Their exact site of origin is unknown. This study incorporated two examples of the ear pommel type (Nos. 510, 512) and two examples of the cotton-reel pommel type (Nos. 509, 513; Fig. 2; Table 1).

Comparable materials to No. 510 have been identified among grave goods from the Talesh cemetery in northwestern Iran (Khalatbari, 2004, Fig. 53) and the Caucasus (Kuftin, 1941, Figs. 59 and 60). The pommel's morphology and decoration, along with the grip and guard forms, closely correspond to No. 512. However, No. 512, which is also an ear-pommel type like No. 510, differs in having a smaller pommel, a circular cross-sectioned grip, and incised lines on the grip. No excavated examples fully replicate No. 512's distinctive features. No. 509 has a comparable counterpart among the Talesh grave goods (Khalatbari, 2004, Fig. 51–11). No. 513, with a disc-shaped pommel slightly larger than No.

Fig. 2. Bronze-hilted iron swords analyzed in this study: (1) No. 509; (2) No. 512; (3) No. 510; (4) No. 513.

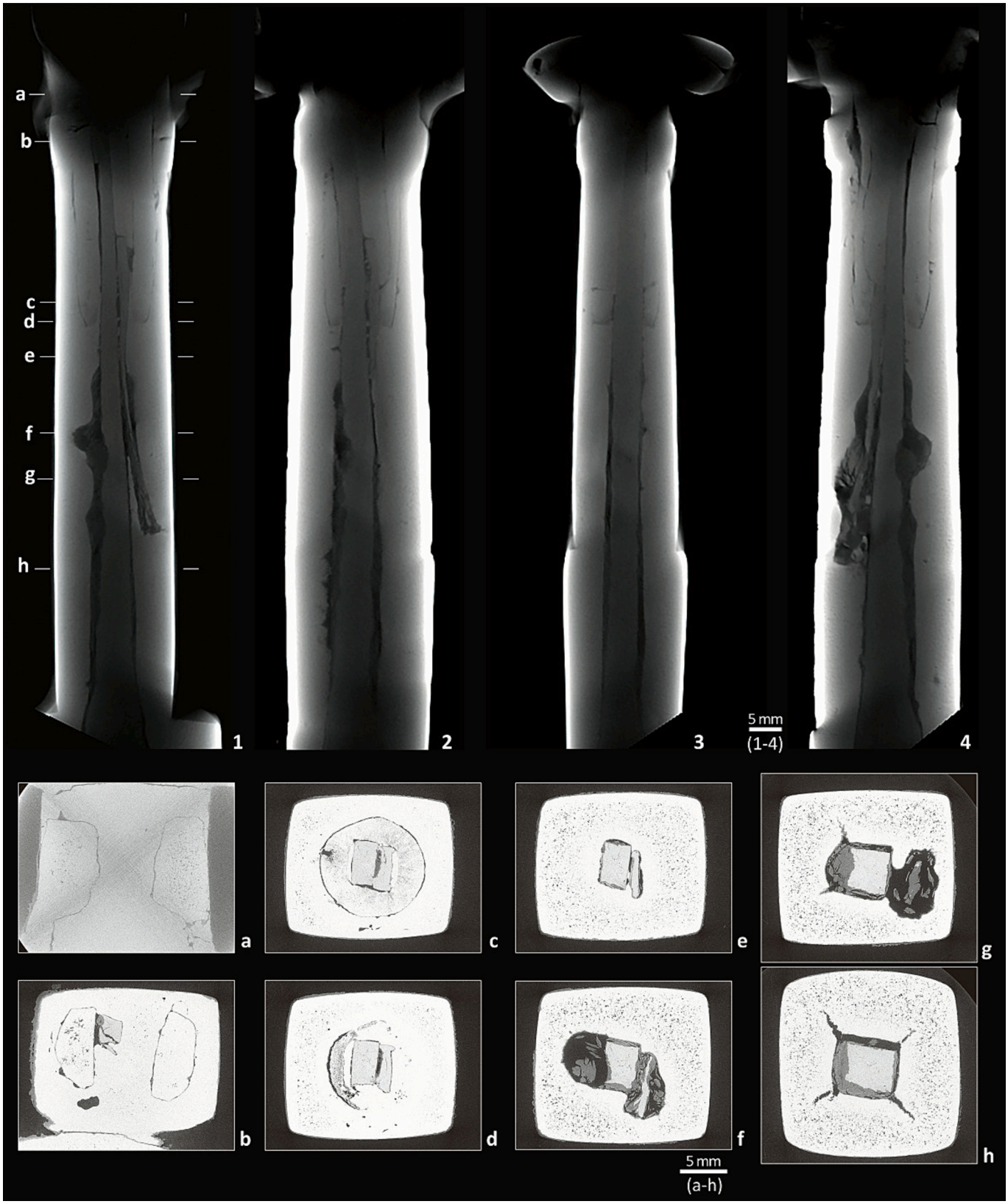

Fig. 3. No. 510: (1, 2, 3, 4) X-ray projection images of the hilt using inspeXio SMX-225CT FRD HR; (a–h) Tomographic sections of the hilt using SPring-8.

509′s, resembles the cotton-reel pommel type from Tomb No. 4 at Ghalekuti II (Fukai and Ikeda, 1971, Pl. XXVII-4, Pl. XLIV-1). The guard's morphology of No. 513 is also similar. Radiocarbon dating and associated inscribed materials date these sites to approximately 1000 BCE (Fukai and Ikeda, 1971, 75, 84–87; Khalatbari, 2004, 15–16).

These pommel types were chosen because a recent neutron analysis did not include the cotton-reel pommel type and indicated that further study was needed of the ear pommel type (Rodzinka et al., 2024, 13).

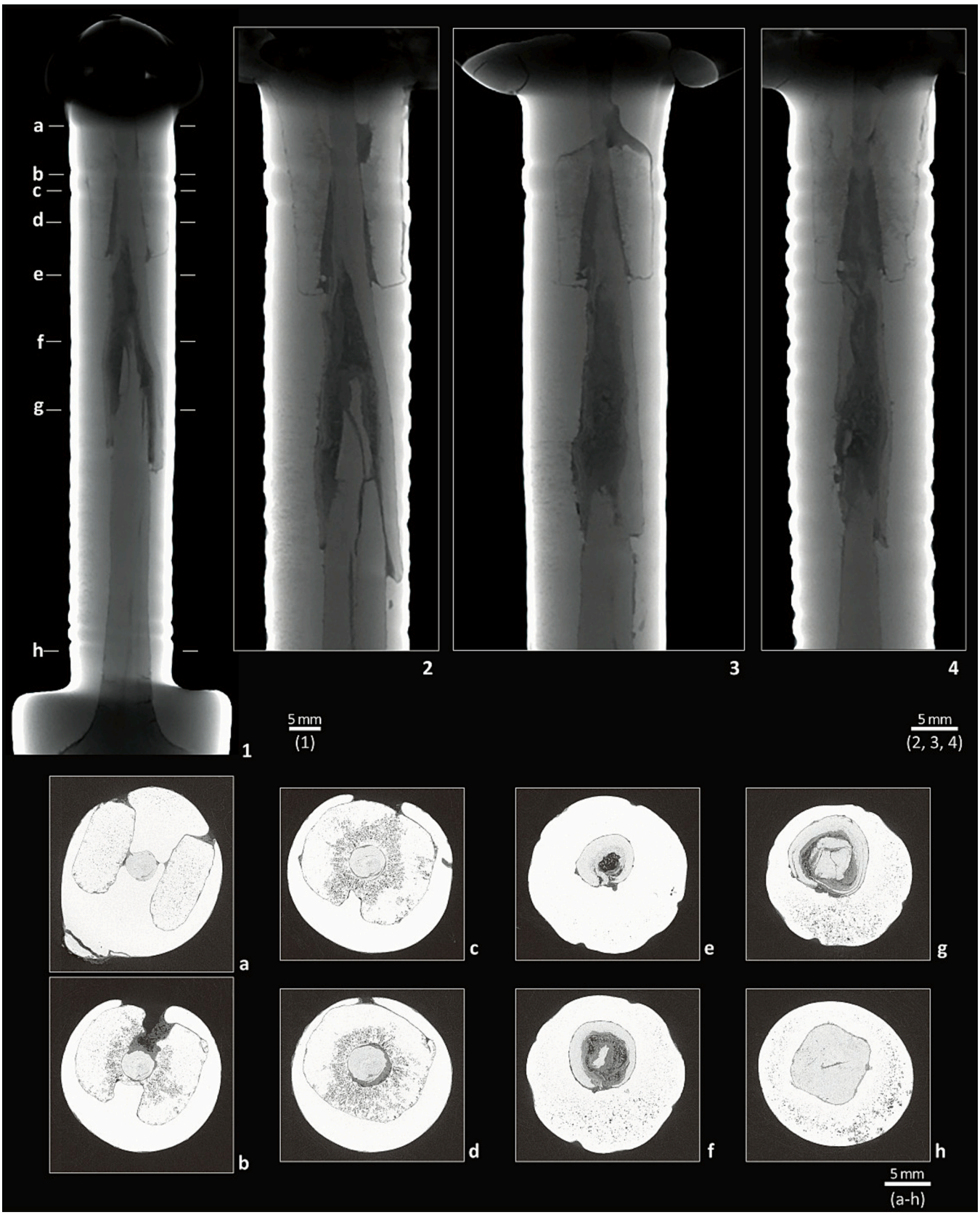

Fig. 4. No. 512: (1, 2, 3, 4) X-ray projection images of the hilt using inspeXio SMX-225CT FRD HR; (a–h) Tomographic sections of the hilt using SPring-8.

Table 1
Bronze-hilted iron swords analyzed in this study.

No.	Pommel type	Length from the top of the pommel to the edge of the guard or blade(mm)	Maximum width of the hilt (mm)	Maximum thickness of the hilt (mm)	Weight (grams)	Figure
509	Cotton-reel	239	75	21	418	2–3
510	Ear	212	81	25	577	2–1
512	Ear	159	48	18	297	2–2
513	Cotton-reel	169	63	16	310	2–4

The current study therefore utilized swords with different pommel types to investigate whether there were internal hilt variations depending on pommel type. All the sword hilts were made of bronze and all exhibited a magnetic reaction extending from the pommel to the guard. It is therefore likely that the iron tangs have survived inside the hilts. Little of the blades remained, and surviving blade material was rusted (Figs. 2-1, 2-2, and 2-3). Rust could also be seen on the inside of the guard and near the guard on hilts with no surviving blade (Figs. 2-4). These findings indicated that the original blades included iron.

Many of the artifacts in previous studies were found to have been modified in later periods, as described above. It has long been indicated that ancient swords have often been modified through the replacement of blades (Wever, 1969). In these, the rusted iron blades were presumably removed over the guard and inside the grip, and bronze blades were inserted (Hajitabar and Haji, 2022; Nojima et al., 2016; Rodzinka et al., 2024). Consequently, traces of putty, petroleum-based paint, and solder are frequently identified around the guard of bimetallic artifacts. In some cases, pommels were partially reconstructed using putty and coated with petroleum-based paint (Nojima et al., 2016). In contrast, the artifacts in this study did not feature replaced blades. Although minor irregular damage was observed near the guard, no evidence of putty, coatings, or solder was found on the pommel or elsewhere. Imaging results revealed no artificial seams or voids. Since their arrival in Japan in the mid-twentieth century, they have been kept in the university as scientific specimens, and no modifications have been made.

Careful consideration is required to determine whether the internal structure, metalwork, and reconstructed production methods of these artifacts reflect ancient techniques. The artifacts show less evidence of significant modification compared with those in prior studies. Their bronze and iron components exhibit characteristic morphologies consistent with excavated materials, suggesting that analytical methods applied here are applicable to similar samples. These findings provide a reference for studying ancient production techniques and a basis for further discussion of bronze-hilted iron swords in the early Iron Age.

3.2. Imaging methods

First, the hilts of the artifacts were imagined using cone beam CT on a microfocus X-ray 3DCT system (inspeXio SMX-225CT FRD HR, Shimadzu Corporation). The X-ray generator's tube voltage was set to 220 kV, with a tube current of 70 μA (μA). The X-ray detector was a 16.4-inch flat-panel detector with an attached copper filter with a thickness of 0.5 mm (mm). The exposure time was set to 1000 ms (msec). The voxel size of the tomography images was 123 μm (μm) for No. 509, 119 μm for No. 510, 107 μm for No. 512, and 123 μm for No. 513. The pommel of No. 513 was enlarged and imaged in three separate sections, for which the X-ray generator was adjusted to a tube current of 120μA. The voxel size was 19 μm. The imaging data were converted to vgl file format and displayed using myVGL (Volume Graphics).

Next, several parts of the hilts were imaged at the synchrotron radiation facility with a ring energy of 8 giga-electron volts at the Japan Synchrotron Radiation Research Institute's (JASRI) SPring-8 facility. The beamline BL28B2 was used, for which a 0.5-mm-thick tungsten plate and a 2.0-mm-thick lead plate are combined to form an absorber, which is used to obtain a high-energy white X-ray spectrum from a bending-magnet source without passing the rays through any optical devices. The X-ray has a peak energy of 200 keV and an energy bandwidth of 100 keV. The X-ray energy was set to 200 keV for the imaging. The detector was a visible-light conversion-type X-ray detector with a digital CMOS board-level camera, C13949-50U (Hamamatsu Photonics K.K.), attached to beam monitor AA60 (Hamamatsu Photonics K.K.). The lens had a focal length of 85 mm (AF-S NIKKOR 85 mm f/1.4G, Nikon). The scintillator that converts X-rays into visible light was a LuAG single-crystal scintillator with a thickness of 500 μm. The distance between the material and the detector was set to 3 m (m), and the distance from the source to the measurement position of the materials was 45 m. The exposure time was set to 40 msec/image, and images were taken at 50 msec intervals.

The imaging was performed using the offset scan method. Each imaging session covered an area with a diameter of approximately 30 mm and a height of approximately 11 mm (1.42 mm × 8 scans). This created 7202 views. The voxel size was 3.99 μm, and the size of the resulting tomography images was approximately 7600 × 7600 pixels in greyscale. In previous similar imaging studies, the voxel size was reported to be 14.8 μm (Hoshino et al., 2017, 3, 7). This study thus featured a higher resolution. The intensity information for the imaging data was saved in a 32-bit floating point format. The processing and display of the data were analyzed using ImageJ (National Institutes of Health).

4. Results

4.1. Ear pommel-type swords

4.1.1. No. 510

This sword had an ear pommel (Fig. 2-1). In the vertical sections, the tang extended from the guard to just below the pommel (Fig. 3-1–4). The horizontal sections of the tang had a square shape near the guard (Fig. 3-g, h) and became flattened near the pommel (Fig. 3-c–e). The width of the tang was 7.5 mm near the guard and 5.3 mm in the middle of the grip.

Along the tang, a flat bar-shaped part (part A) could be observed (Figs. 3-1, 3-4, 3-c–g). Part A was apparently forge welded to the tang, but space between it and the tang existed and became wider near the guard (Fig. 3-g). The forge welding was likely done improperly. At the cross-section where the tang and part A were most closely connected, they appeared to be fixed by a cylindrical part, or part B (Fig. 3-c, d). Part B was likely made of bronze. Interestingly, part B appeared to split into two branches near the pommel (Figs. 3–4, 3-b). The split blanches gradually widened and appeared to connect to the saddle-shaped arch in the center of the pommel (Fig. 3-a, b). If this was the case, part B was a part of the pommel and likely fixed the tang to the pommel. In the cylindrical part of part B, there was another thin metal layer outside the tang and part A, and these were joined tightly (Fig. 3-c, d).

The grip was formed by bronze casting, probably after the iron tang was fixed with the above parts. No seams were observed in the bronze casting; the bronze was likely poured in a single operation. Joint lines were observed along the rims in a cross-section of the pommel (Fig. 3-a), indicating that they may have been cast jointed to the saddle-shaped arch. Further examination is necessary as the imaging of this pommel was unclear.

The bronze was in good condition overall. Inside the bronze, fine voids—probably originating from the pouring process—were observed.

The inside of part A showed relatively more bubbles than the outer casting bronze (Fig. 3-c, d). This would allow a future analysis of the difference in the pouring conditions of the bronze.

4.1.2. No. 512

This sword has an ear pommel (Fig. 2-2). CT images confirmed that the iron tang extended continuously from the guard to the grip (Fig. 4-1). The horizontal section of the tang was circular, resembling a rounded square (Fig. 4-g, h). The diameter was 7.5 mm near the guard and 6.6 mm at the middle of the grip. The tang tapered toward the pommel and ceased at the middle of the grip. It did not reach the pommel (Figs. 4-1–4, 4-e–h).

The tang was joined to another part (part C) at the middle of the grip (Figs. 4-1–4, 4-f–h). Part C was foil-like and wrapped around the tang (Fig. 4-e–g). It was 1.8 mm thick. The tang ended near the pommel, leaving only part C (Fig. 4-e), which was here twisted into a bar shape (Figs. 4-1–4, 4-a–d). The bar-shaped part C extended to the pommel. The outer surface of the pommel featured a rusted circular area at the top. This was thought to correspond to the top of part C. Since this area was magnetized, part C was believed to contain iron. Another cylindrical part (part D) was joined at the point where part C formed the bar shape (Fig. 4-d). Part D gradually split into two branches toward the pommel (Fig. 4-b, c). The two branches of part D appeared to be connected to saddle-shaped part of the pommel (Fig. 4-a).

A lack of seams in the bronze of the guard and the grip indicated that the bronze was poured in a single operation, much like No. 510. The rims of the pommel seem to be cast joints to the saddle-shaped part. Fine voids, which likely originated during pouring, were apparent within the bronze. Relatively many bubbles were observed inside part D (Fig. 4-a–d). There were misruns around the pommel (Fig. 4-a–c) and on the edges of the guard (Fig. 2-2). No significant defects or flaws were found inside the bronze.

4.2. Cotton-reel pommel-type swords

4.2.1. No. 509

This sword had a cotton-reel pommel (Figs. 2-3). In the vertical sections, the tang extended from the guard to the pommel (Fig. 5-1–4). The horizontal section of the tang was unevenly square. The long side of the section was 8.5 mm near the guard and 5.3 mm in the middle of the grip. Interestingly, there seemed to be space around the tang in the grip (Fig. 5-1–4). The bronze covering the grip was thin and tubular (Fig. 5-a, 5-e–h). The thickness of the bronze varied from 1.5 to 5.5 mm. A close look at the outer surface of the grip showed that light-brown lumps were “attached” in some places (Figs. 6-1, 6-2). At the cross section where the lumps could be observed, small holes had opened in the outer bronze casting; it appears that these “attachments” were emerging from inside the grip (Fig. 6-a). They appeared to be made of sand- or clay-like material, perhaps molding or foundry sand. This material likely was used to fill the space between the iron tang and the outer bronze casting.

In the middle of the pommel, between the two disks, the iron tang was in contact with the bronze. Here, there were two layers of bronze casting (Fig. 5-b–d). Bronze was thus poured twice. Overall, fine voids were apparent within the bronze of the grip and were particularly abundant in the guard (Fig. 5-1). In the two bronze layers in the pommel, more fine gas seems to have been generated in the bronze by the first pouring (Fig. 5-b–d). These defects, which seem to have formed during the pouring, may also be related to the coarse casting surface of the grip.

4.2.2. No. 513

This sword had a cotton-reel pommel (Figs. 2-4). On the external surface of the guard, the crack was repaired by metallic wax. No traces of repairs were apparent. In the vertical sections, the iron tang extended from the guard to the pommel (Fig. 7-1–4). The tang had a complex morphology. Near the guard, the horizontal section of the tang was flat and square (Fig. 7-h). The long side of the section was 6.3 mm. In the middle of the grip, the section of the tang was square with rounded corners, with one side being 5.2 mm. Near the pommel, the section was almost circular, with a diameter of 4.4 mm (Fig. 7-e). Near the guard, the tang was joined to a flat iron piece with a nail (Fig. 7-f, g). Inside the pommel, it appeared to be joined with a new bar-shaped piece and twisted (Fig. 7-d, e).

The bronze covering the grip was thin and tubular in shape (Fig. 7-1–4). The thickness was 1.4 mm and uniform. A clay-like material likely to covered the iron tang within the grip (Fig. 7-f, g). The same material seemed to fill the interior of the thicker disc of the pommel. Otherwise, the internal structure of the pommel differed from that of the grip. A foil-like piece (part E) was wrapped around the tang multiple times, occasionally forming layers (Fig. 7-a–e, 8). In the tomography images of the pommel taken with the microfocus X-ray CT system, the tang extended to the middle of the pommel, between the two discs (Fig. 8-e, f). However, the tang was disconnected in the upper half of the pommel (Fig. 8-d). At the point where the tang ended, part E became bar-shaped and was wrapped by another foil-like piece (Fig. 8-a–c). A projection covered with bronze extended from the top of the outer surface of the pommel, which was likely the end of the bar-shaped part E. This projection was magnetic, suggesting that part E contained iron.

At the pommel where part E was wrapped around the tang, the bronze directly covered part E. However, near the middle of the pommel, the clay-like material partially covered part E (Fig. 7-a, b). This corresponded to the point at which the tang ended. Some of the clay-like material had peeled away from part E, likely when the bronze was poured (Fig. 7-a, b). The bronze formed thin layers near the pommel, suggesting that it was poured several times (Fig. 7-d, e). A seam could be observed in the bronze at one of the four convex bands on the pommel (Fig. 8-e). These bands were for both decoration and would have concealed the traces of production. The pommel was formed by cast jointing several times, and the foil-like part E was likely applied in accordance with the pouring.

Fine cavities were observed within the bronze. They were particularly numerous in areas where the bronze covering the pommel was thicker (Fig. 7-c). Some parts resembling shrinkage cavities were also scattered inside the bronze. In addition, large cavities formed inside the bronze in the guard where the blade survived (Fig. 7-1).

5. Discussion

The high-resolution tomographic images of the bronze-hilted iron swords revealed variations in the internal structure and thus their production techniques. These variations partially corresponded to pommel type. First, the swords with ear pommel featured joints with unique bronze parts (parts B and D) for the iron tangs. These parts were part of the pommels. The tangs did not penetrate the pommels. Parts B and D seem to have been the cores for modelling the pommels. Further consideration is needed to determine whether these parts were poured directly onto the tang or made separately. The bronze casting from the guard to the grip was performed in a single operation after combining these parts.

The bronze-hilted iron swords with cotton-reel pommel also exhibited distinct manufacturing techniques. The bronze was not cast directly onto the iron tang. Instead, the tang was covered with a sand- or clay-like material that may have been made of a substance like foundry sand. The bronze covering the grip was likely then poured over it. The bronze casting was thin, being less than 5 mm thick in some places. On the pommels, the bronze was poured more than once.

Careful consideration is required to determine whether the results genuinely represent “ancient” technology. While this remains hypothetical, variations according to pommel type were to be taken as reflecting different production techniques, there may have been systematic differences in the methods of combining different metals, as seen in the bronze casting methods around the iron tang. In the ear pommel-type swords, bronze casting was done directly on the iron tangs.

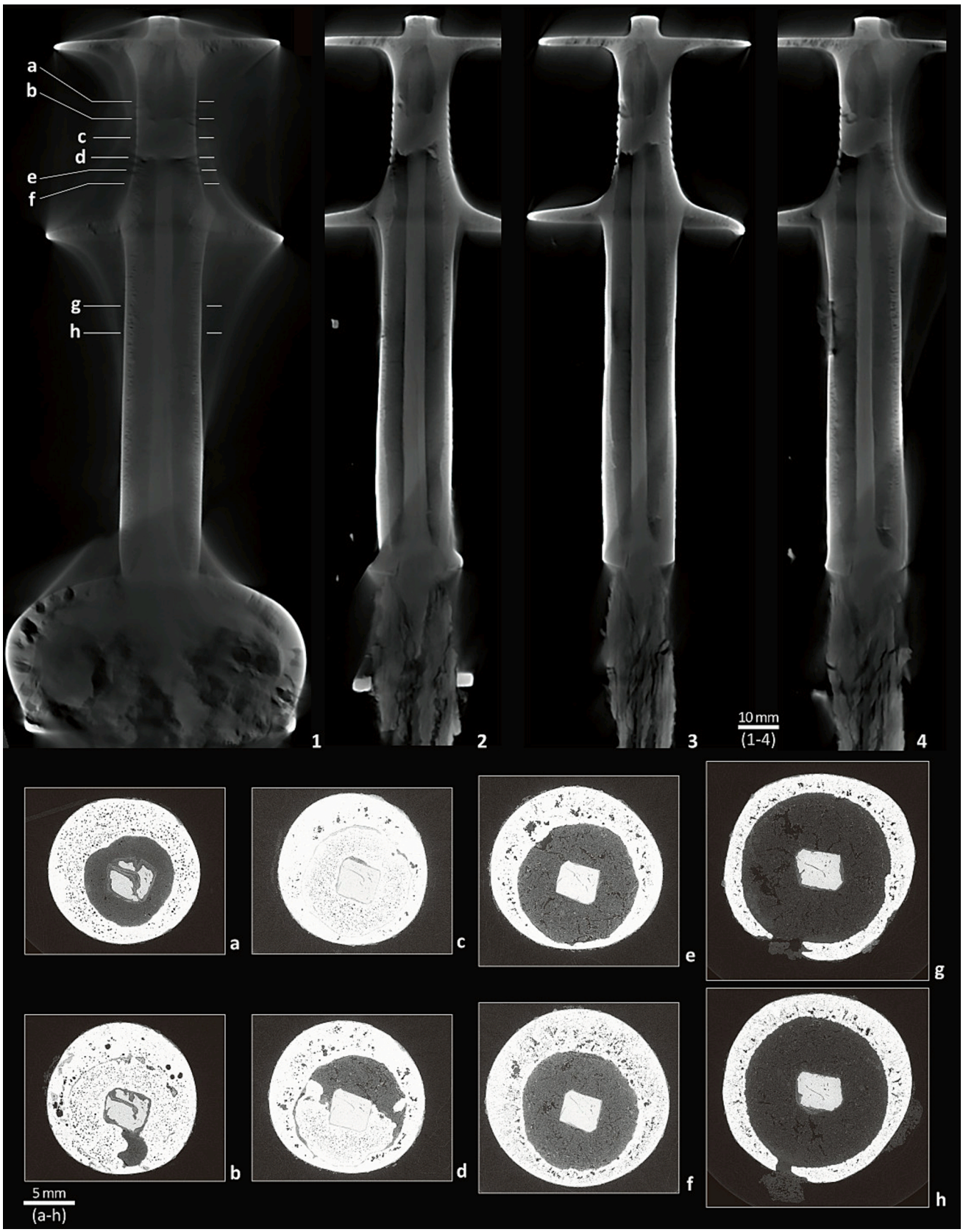

Fig. 5. No. 509: (1, 2, 3, 4) X-ray projection images of the hilt using inspeXio SMX-225CT FRD HR; (a–h) Tomographic sections of the hilt using SPring-8.

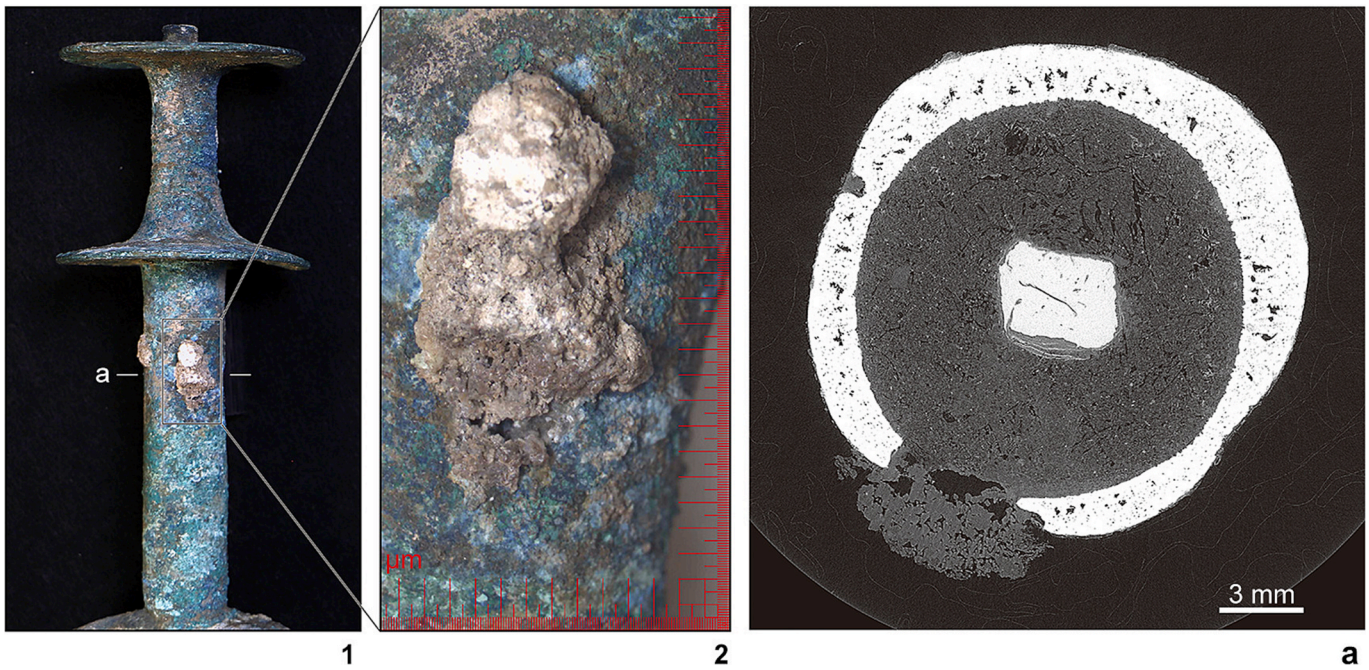

Fig. 6. Details of No. 509: (1) The hilt; (2) "Attached substances" on the hilt's outer surface; (a) Tomographic section at the solid line shown in (1) using SPring-8.

Although No. 512 shows some defects in the bronze, these were likely due to the complexity of the morphology rather than the failure of the insert. Moreover, almost no serious cavities were apparent in the contact surfaces of the bronze and iron. The gas inside the bronze was well controlled.

In contrast, in the cotton-reel pommel-type swords, techniques like casting bronze onto iron and welding the two metals together were practically not used. Here, a clay-like material mediated the contact between iron and bronze, and the bronze casting was thin. Notably, the tomographic image of the cotton-reel pommel-type sword excavated at Ghalekuti II aligns with these observations (Okayama Orient Museum et al., 2017, Fig. 3). The bronze parts, especially on the pommels, appeared to be cast jointed and formed through tinkering rather than pouring. This hilt structure would have been weaker. The fixation of the blade and hilt would lack stability. This production technique may have been due to a relative lack of skill in casting bronze directly onto iron. Additionally, large voids were apparent inside the bronze on the surfaces in contact with the iron and the two metals were not sufficiently welded. This may indicate differences in the degree of proficiency in the production techniques of iron–bronze bimetal tools in the early phase of iron adoption.

Meanwhile, common features between the two types were identified. The hilts were not made simply with integral casting. The pommels were all likely formed through multiple pouring or cast joints. Additionally, before casting the pommels, some parts were fixed to the tangs. During that process, foil-shaped parts (parts C and E) were used for both types. The function and necessity of these parts require further investigation, but may have served as a core for casting the pommels. Although they likely contained iron, it was minimal and probably could not withstand hot forging. Rather, it was likely wrapped onto the tangs by cold forging. These parts must have different hardness and properties from those used for the tangs and blades. If so, this indicates that metalworkers in the early Iron Age may have already been able to control iron's carbon content to some extent. It is also possible that they used multiple types of raw iron materials, which would reflect knowledge of these materials' properties, weaknesses, and strengths. Meanwhile, the foil parts do not seem to have been forge-welded to the iron tangs. This may reflect technical limitations in ironworking technology, as the use of the foil-like parts could have represented an attempt to overcome such limitations.

6. Conclusions

This study has further demonstrated the potential for high-energy X-ray imaging in analyzing the structure of bronze-hilted iron swords in non-destructive way. The high-resolution tomography images revealed complex internal structures, including within the iron and bronze. The results merit cautious interpretation to confirm their reflection of ancient technology. Nevertheless, they offer preliminary insights into bimetallic artifacts manufacturing and warrant further investigation using artifacts with clear archaeological provenance. Consistent imaging data from excavated materials support the potential of this study's data to contribute to analyzing comparable artifacts and formulating hypotheses.

The differences within the hilts demonstrated that variations in production techniques may have existed and been associated with the type of pommel used. Furthermore, certain morphological features of the pommel and grip that have been regarded as design elements are also possibly related to production techniques. If these findings are confirmed with further study using reliable contextual materials, it would allow a more consistent estimation of internal structure based on morphological features. It would also be possible to better reconstruct the regional evolution of metallurgical techniques during iron adoption, as well as their limitations and complementary techniques. The practices presented in this study could also be used in the analysis and interpretation of similar materials. Future research should incorporate AMS radiocarbon dating of preserved iron tangs, metallographic studies of iron and copper or bronze components, and lead isotope analysis of bronze hilts. These methods will enable more robust interpretations of early iron metallurgy in northern Iran and the South Caucasus.

Northern Iran and the South Caucasus are known for their large quantity of surviving ancient metal artifacts. Their quality and locality suggest that the local people were well skilled in working with bronze. Moreover, each region experienced unique innovations and various trials in the adoption process of iron. This study presented an effective method and hypotheses for future research into how and why iron was put into practical use and gradually became more widely adopted.

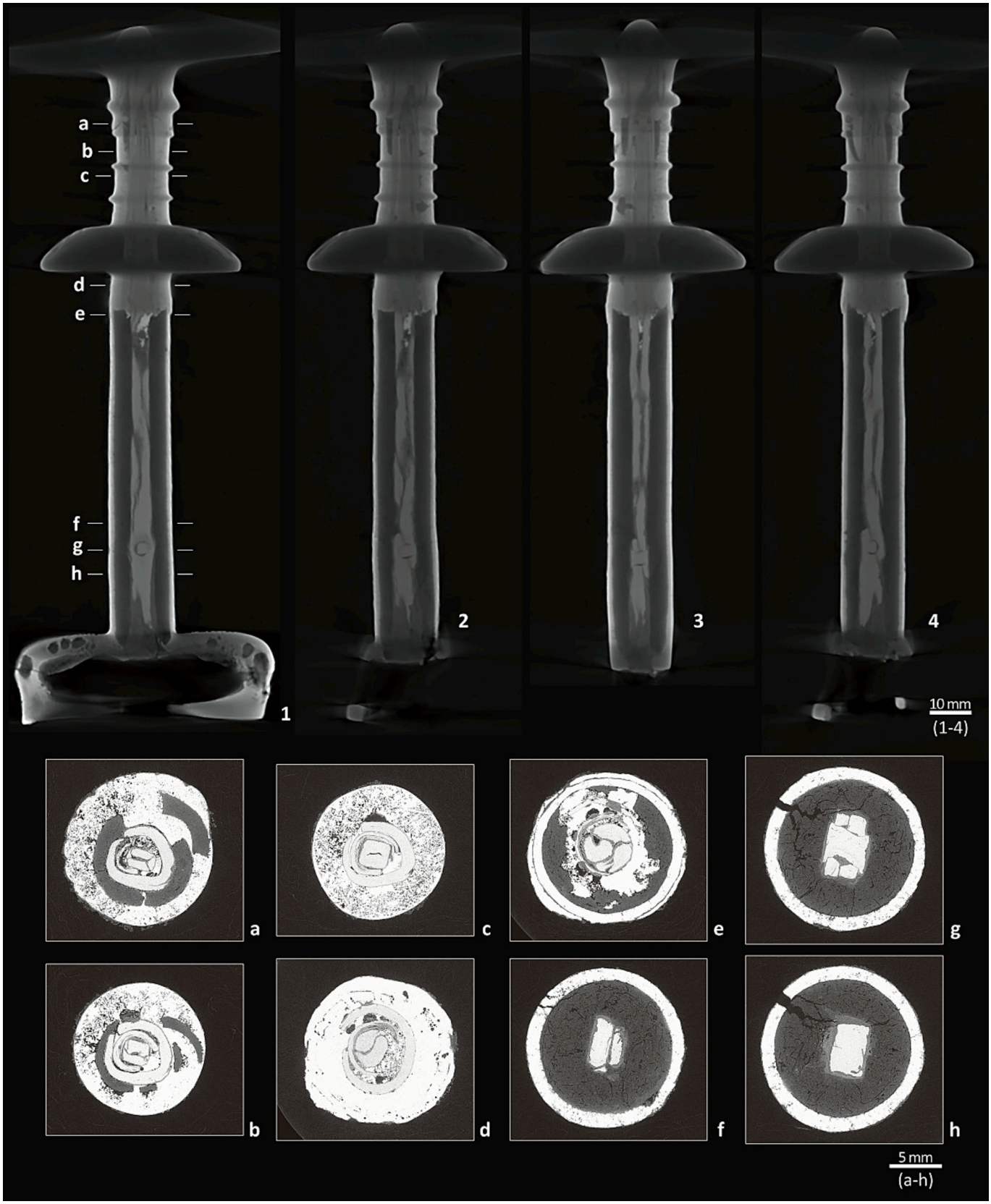

Fig. 7. No. 513: (1, 2, 3, 4) X-ray projection images of the hilt using inspeXio SMX-225CT FRD HR; (a–h) Tomographic sections of the hilt using SPring-8.

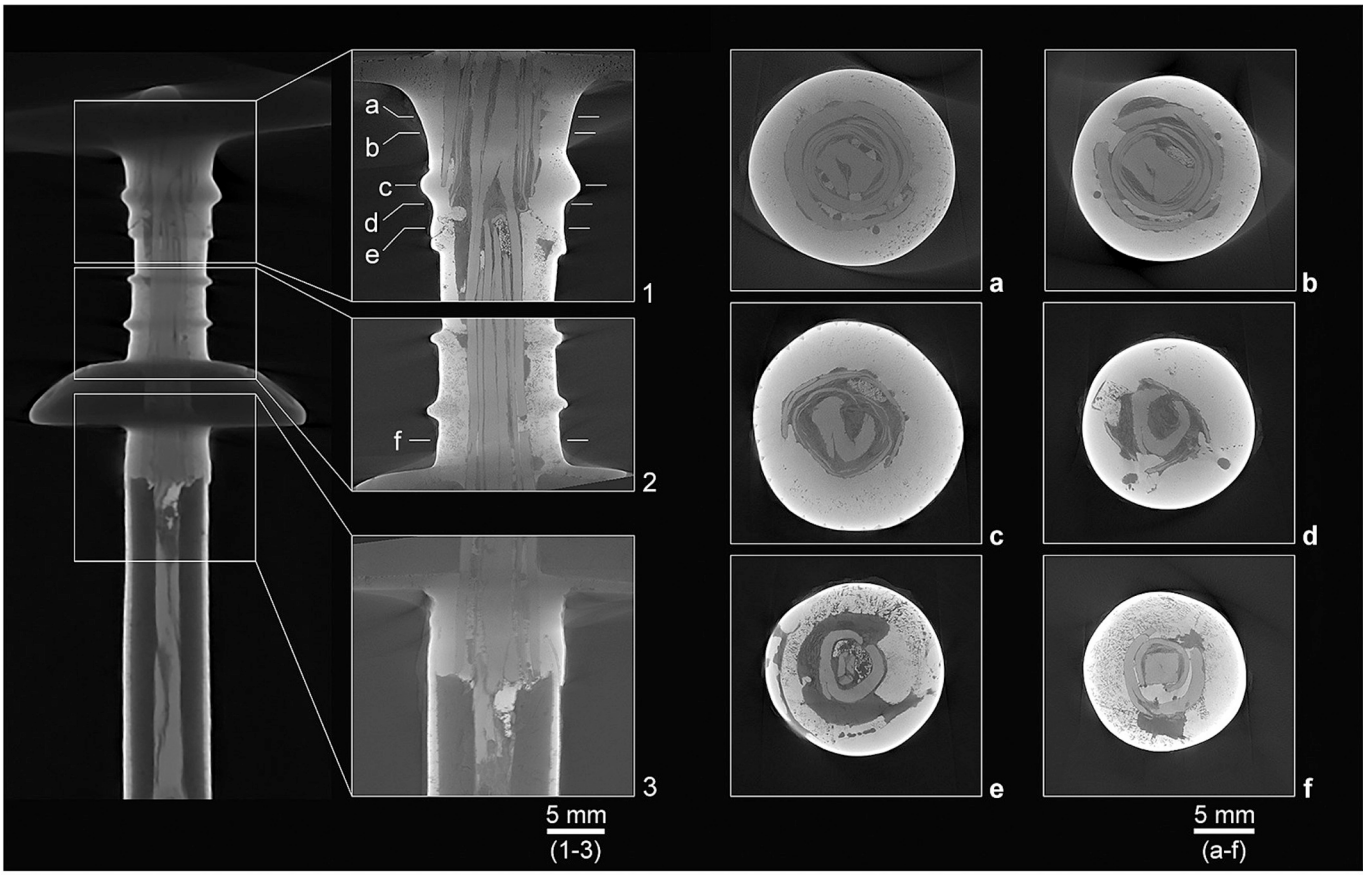

Fig. 8. Pommel of No. 513: (1–3) X-ray projection images using inspeXio SMX-225CT FRD HR; (a-f) Tomographic sections using inspeXio SMX-225CT FRD HR.

7. Glossary

High-energy X-ray imaging: A technology that uses high-energy X-rays, with energy of several keV (kiloelectron volts) or more, to visualize the internal structure of materials without destroying them. These high-energy X-rays have higher penetrating power than conventional X-rays, enabling internal observation of thick samples and high-density materials with spatial resolution at the μm level.

Iron Age: The Iron Age in northern Iran primarily corresponds to the period from the middle of the second millennium BC to the middle of the first millennium BC, based on pottery chronology.

Author contributions

Yui Arimatsu was responsible for conducting the research activity and securing the necessary resources, including funding. Yui Arimatsu designed the study, developed the main conceptual framework and proof outline, collected data, and drafted the manuscript.

Funding source

This work was supported by the Fusion Oriented Research for Disruptive Science and Technology, Japan Science and Technology Agency (Grant No. JPMJFR2271).

CRediT authorship contribution statement

Yui Arimatsu: Writing – review & editing, Writing – original draft, Visualization, Validation, Supervision, Software, Resources, Project administration, Methodology, Investigation, Funding acquisition, Formal analysis, Data curation, Conceptualization.

Declaration of Competing Interest

The authors declare that they have no known competing financial interests or personal relationships that could have appeared to influence the work reported in this paper.

Acknowledgements

Mukai Yusuke (Associate Professor of Kyoto University) kindly permitted the analysis of the materials for the study. Nojima Hisashi (Professor of Hiroshima University) provided precious advice on various matters. The analysis was conducted with the invaluable cooperation and support of Nakayama Takashi and Rikura Takahiro (experts at Shimadzu Techno-Research, Inc.).

Data availability

Data will be made available on request.

References

Danti, M.D., 2013. The late bronze and early Iron Age in northwestern Iran. In: Potts, D. T. (Ed.), The Oxford Handbook of Ancient Iran. Oxford University Press, Oxford, pp. 327–376.

Drescher, H., 1958. Der überfangguss: Ein Beitrag zur vorgeschichtlichen Metalltechnik. Verlag des Römisch-Germanischen Zentralmuseums, Mainz.

de Morgan, J., 1927. La Prehistoire Orientale, 3. Paul Geuthner, Paris.

Eliyahu-Behar, A., Yahalom-Mack, N., Shilstein, S., Zukerman, A., Shafer-Elliott, C., Maeir, A.M., Boaretto, E., Finkelstein, I., Weiner, S., 2012. Iron and bronze production in Iron Age IIA Philistia: New evidence from Tell es-Safi/Gath. Israel. J. Archaeol. Sci. 39, 255–267. https://doi.org/10.1016/j.jas.2011.09.002.

Erb-Satullo, N.L., 2019. The innovation and adoption of iron in the ancient near east. J. Archaeol. Res. 27, 557–607. https://doi.org/10.1007/s10814-019-09129-6.

Erb-Satullo, N.L., Jachvliani, D., Kakhiani, K., Newman, R., 2020. Direct evidence for the co-manufacturing of early iron and copper-alloy artifacts in the Caucasus. J. Archaeol. Sci. 123, 105220. https://doi.org/10.1016/j.jas.2020.105220.
Fukai, S., Ikeda, J., 1971. Dailaman IV: the Excavation at Ghalekuti II & I, 1964. The University of Tokyo, Tokyo, The Institute of Oriental Culture.
Gambaschidze, I., Hauptmann, A., Slotta, R., Yalçin, Ü. (Eds.), 2001. Georgien: Schätze aus dem Land des goldenen Vlies; Katalog der Ausstellung des Deutschen Bergbau-Museums Bochum in Verbindung mit dem Zentrum für Archäologische Forschungen der Georgischen Akademie der Wissenschaften Tbilissi vom 28. Oktober 2001 bis 19. Mai 2002. Deutsches Bergbau-Museum.
Hajitabar, M., Haji, M., 2022. Typology of swords called ear pommel swords in Iron Age II in Iran based on the collections of Mostazafan Foundation's museums. Anc. Iran. Stud. 1, 41–66. https://doi.org/10.22034/AIS.2022.146348. (in Persian with English abstract).
Hoshino, M., Uesugi, K., Shikaku, R., Yagi, N., 2017. High-energy, high-resolution x-ray imaging for metallic cultural heritages. AIP Adv. 7, 105122. https://doi.org/10.1063/1.5003162.
Japan Synchrotron Radiation Research Institute (JASRI), 2017. SPring-8 research highlight no. 103. SPring-8. http://www.spring8.or.jp/ja/news_publications/research_highlights/no_103/ (in Japanese).
Khalatbari, M.R., 2004. Archaeological Investigations in Talesh, Gilan. 1. Excavations at Toul-e Gilan. General Office of Iranian Cultural Heritage Organization, Tehran.
Kontani, R., 2001. Reconsideration of ancient Iranian bimetallic swords. Bull. Okayama Orient Mus. 18, 21–30.
Kontani, R., Tanaka, H., 2002. Restoring the bronze swords with iron cores in northwerstern Iran: an inquiry into bimetal technique. Bull. Okayama Orient Mus. 19, 39–50.
Kontani, R., 2005. Searching for the origin of the "bronze swords with iron core" in northwestern Iran and the Caucasus region. Iran. Antiq. 40, 397–421. https://doi.org/10.2143/IA.40.0.583218.
Kuftin, B.A., 1941. Archaeological Excavations in Trialeti I: An Attempt to Periodize Archaeological Materials. Academy of Sciences of the Georgian SSR. (in Russian).
Moorey, P.R.S., 1974. Ancient Bronzes from Luristan. British Museum, London.
Maxwell-Hyslop, K.R., Hodges, H.W.M., 1962. Bronzes from Iran in the collections of the Institute of Archaeology, University of London (with a technical report on the bronzes by H. W. M. Hodges). Iraq 24, 126–133. https://doi.org/10.2307/4199723.
Medvedskaya, I.N., (translated by Pavlovich, S.) 1982. Iran: Iron Age I. BAR International Series 126. BAR Publications, Iran.
Nieling, J., 2009. Die Einfuhrung Der Eisentechnologie in Sudkaukasien Und Ostanatolien Wahrend Der Spatbronze- Und Fruheisenzeit (Black Sea Studies, Band 10). Aarhus University Press, Aarhus.
Nojima, H., Arimatsu, Y., Fujii, M., Murata, S., Ichikawa, H., Fujii, S., Morimoto, N., 2016. Bronze-hilted iron swords from western Asia at the department of archaeology, Hiroshima University. Bull. Hiroshima Univ. Archaeol. Lab. 8, 1–32. https://doi.org/10.15027/42467.
Okayama Orient Museum, Hiroshima University, Synchrotron Radiation Research Institute, 2017. An ancient high-tech product combining two types of metals: Visualization of making technique of bimetallic sword by using SPring-8. Press Release. http://www.spring8.or.jp/ja/news_publications/press_release/2017/170216/ (in Japanese).
Pigott, V.C., 1981. The adoption of iron in western Iran in the early first millennium B. C: An Archaeometallurgical Study. Ph.D. Dissertation, Dept. of Anthropology, University of Pennsylvania, University Microfilms International, Ann Arbor.
Pigott, V.C., 1989. The emergence of iron use at Hasanlu. Exped. Mag. 31, 67–79.
Pigott, V.C., 1999. The development of metal production on the Iranian Plateau: an archaeometallurgical perspective. MASCA Research Papers in Science and Archaeology 16, 73–106.
Pigott, V.C., 2004. Hasanlu and the emergence of iron in early 1st millennium BC western Iran. In: Stollner, T., Slotta, R., Vatandoost, A. (Eds.), Persiens Antike Pracht: Bergbau. Handwerk, Archaeologie, Deutsches Bergbau-Museum, pp. 350–357.
Rodzinka, A.E., Fedrigo, A., Scherillo, A., Shortland, A.J., Simpson, S.J., Erb-Satullo, N. L., 2024. Neutron tomography reveals extensive modern modification in Iron Age Iranian swords. J. Archaeol. Sci. 171, 106018. https://doi.org/10.1016/j.jas.2024.106018.
Shizuma, K., Kajimoto, T., Endo, S., Matsugi, K., Arimatsu, Y., Nojima, H., 2017. Non-destructive analysis of ancient bimetal swords from western Asia by γ-ray radiography and X-ray fluorescence. Nucl. Instrum. Methods Phys. Res. B 407, 244–255. https://doi.org/10.1016/j.nimb.2017.07.014.
Simpson, S.J., La Niece, S., 2010. New light on old swords from Iran. Br. Mus. Tech. Res. Bull. 4, 95–101.
Thornton, C.P., Pigott, V.C., 2011. Blade-type weaponry of Hasanlu period IVB, in: de Schauensee, M., Dyson, R.H. (Eds.), Peoples and Crafts in Period IVB at Hasanlu, Iran, University of Pennsylvania Museum of Archaeology and Anthropology, Pennsylvania, pp. 135–182.
Waldbaum, J.C., 1982. Bimetallic objects from the eastern Mediterranean and the question of the dissemination of iron. In: Muhly, J.D., Maddin, R., Karageorghis, V. (Eds.), Acta of the International Archaeological Symposium on Early Metallurgy in Cyprus, 4000-500 BC. Pierides Foundation, Larnaca, pp. 325–349.
Wever, G., 1969. A Persian puzzle: a bronze sword from Tehran. Expedition 12, 24–27.
Yahalom-Mack, N., Eliyahu-Behar, A., 2015. The transition from bronze to iron in Canaan: Chronology, technology, and context. Radiocarbon 57, 285–305. https://doi.org/10.2458/azu_rc.57.18563.